Title

JARID1-targeted histone H3 demethylase inhibitors exhibit anti-proliferative activity and overcome cisplatin resistance in canine oral melanoma cell lines

Journal

Veterinary and Comparative Oncology, 19(3)

ISSN

1476-5810

Authors

Tobin, Savannah J
Chang, Hong
Kent, Michael S
et al.

Publication Date

2021-09-01

DOI

10.1111/vco.12691

Peer reviewed

HHS Public Access

Author manuscript

Vet Comp Oncol. Author manuscript; available in PMC 2021 September 21.

Published in final edited form as:

Vet Comp Oncol. 2021 September ; 19(3): 518–528. doi:10.1111/vco.12691.

JARID1-targeted histone H3 demethylase inhibitors exhibit anti-proliferative activity and overcome cisplatin resistance in canine oral melanoma cell lines

Savannah J. Tobin[1,2], **Hong Chang**[2], **Michael S. Kent**[2], **Alexander E. Davies**[1]

[1]Department of Veterinary Biosciences, College of Veterinary Medicine, The Ohio State University, Columbus, Ohio

[2]Department of Surgical and Radiological Sciences, School of Veterinary Medicine, University of California Davis, Davis, CA

Abstract

Histone demethylases are overexpressed or display altered activity in numerous human cancers leading to alterations in cell cycle dynamics, DNA repair kinetics, and therapeutic resistance. Consequently, therapeutic targeting of histone demethylases has become an active and promising area of research in human oncology. However, the role of histone demethylases and the potential efficacy of demethylase inhibition in canine cancers remains largely unknown. In the present work, we addressed this knowledge gap by exploring the therapeutic potential of histone demethylase inhibitors (HDIs) in canine oral melanoma. Using canine melanoma cell lines, we determined that broad spectrum HDIs result in decreased cell survival and prolonged DNA damage repair kinetics. We then showed that JARID1B, a histone H3 demethylase implicated in proliferation-dormancy regulation and drug sensitivity in human cancers, is highly expressed in canine tumour tissues. HDIs targeting JARID1B, and related JARID1 family members, significantly reduced survival fractions in canine melanoma cell lines, but did not appear to modulate DNA damage repair kinetics like broad spectrum HDI treatments. Importantly, we found that the anti-proliferative effects of JARID1-targeted HDIs are preserved in cell lines resistant to platinum-based chemotherapeutics, suggesting that HDIs may serve as a viable therapeutic strategy when faced with oral melanomas that progress despite the use of conventional therapies.

Keywords

DNA damage; drug resistance; H3K4; H3K9; KDM5

Correspondence: Alexander E. Davies, Department of Veterinary Biosciences, College of Veterinary Medicine, The Ohio State University, Columbus, OH 43210, USA. davies.474@osu.edu.

CONFLICT OF INTEREST

The authors declare no competing interests.

DATA AVAILABILITY STATEMENT

Data will be made upon reasonable request to the corresponding author.

SUPPORTING INFORMATION

Additional supporting information may be found online in the Supporting Information section at the end of this article.

1 | INTRODUCTION

Melanoma is the most common malignant oral tumour in the dog.[1] Patients frequently present late in the course of disease with large, invasive, oral lesions that are incompletely resectable and have often metastasized. Treatment regularly consists of combinations that include ionizing radiation, the melanoma vaccine, and/or systemic chemotherapy using platinum-based agents. However, treatment options are usually not curative and despite intervention, patients still die from metastatic disease.[2–4] Therefore, new approaches that increase treatment efficacy are much-needed.

Standard therapeutic approaches for canine melanomas, and other cancers, focus on killing rapidly dividing tumour cells through the induction of DNA damage using ionizing radiation and/or cytotoxic drugs.[5] However, the efficacy of these approaches is dependent upon many factors including cell proliferation dynamics, chromatin condensation states, and the expression/activity relationships of enzymes required for DNA damage repair.[6,7] All of these factors are regulated by histone modifying enzymes which exert cellular function through the dynamic addition or removal of post-translational modifications (PTMs), such as acetyl and methyl groups on histone tails.[8] While acetylation usually results in transcriptional activation, methylation can lead to gene activation or repression depending on the specific residue modified, the number of methyl groups appended, or interactions with other PTMs and DNA-binding proteins.[9] For example, methylation at H3 lysine 4 (H3K4) is generally an activating modification that results in increased transcription, while methylation at H3K9 or H3K27 often results in compressed heterochromatin and transcriptional repression.[6] As such, dysregulation of histone demethylase activity dynamics can alter cell cycling rates, inhibit the intercalating capacity of drugs, and modulate DNA repair enzyme expression/function through altered chromatin states that favour tumour survival.[10–14] Thus, the broad functions of histone demethylases can have a profound impact on the clinical effectiveness of standard therapeutic approaches in melanoma and other cancers.

Although many histone demethylase enzymes function as key modulators of cellular processes relevant to cancer progression and treatment, the JARID1/KDM5 family (JARID1A/1B/1C/1D) of histone demethylases may play an especially important role in the sensitivity of melanoma cells to therapy. The JARID1 family of demethylases serve as transcriptional corepressors that selectively target di- and trimethylated H3K4. Through these activities, they are linked to diverse processes such as regulating G1-S progression, PI3K/AKT signalling, epithelial to mesenchymal transition, metastasis, and the acquisition of slow-cycling cancer stem cell (CSC)-like states that are drug resistant.[10,15–17] Specifically, JARID1B has been associated with CSC-like states and drug resistance in human melanoma.[10,11] Other classes of demethylases may have cooperative effects with JARID1 family members, such as H3K9 demethylases JMJD1A/KDM3A and JMJD2B/KDM4B. Upregulation of H3K9 demethylases has also been shown to enhance DNA damage repair kinetics conferring radiation and cytotoxic drug resistance.[12,18] Altogether, these reports suggest that inhibiting JARID1 family members and other histone demethylases in cancer may provide an opportunity to enhance the efficacy of existing therapeutics. However, demethylase expression and function are still poorly understood in canine melanoma and other canine cancers.

Herein, we hypothesized that histone demethylase activity represents a targetable mechanism for anti-cancer treatment that can be applied to canine oral melanomas. The first objective of this study was to investigate the therapeutic potential of broad-spectrum histone demethylase inhibitors alone, or in combination with existing treatment approaches including cytotoxic agents or ionizing radiation. The second objective was to determine if the drug resistance-associated JARID1 family of histone demethylases are expressed in canine melanoma and targetable to reduce survival and/or overcome resistance to standard chemotherapeutic agents.

2 | MATERIALS AND METHODS

2.1 | Cell culture and cell line validation

Canine oral melanoma cell lines UCDK9M2 and UCDK9M4 (RRID: CVCL_0C78 and CVCL_0C80) were provided by Dr. Michael Kent (University of California, Davis, CA, USA).[19,20] Jones oral canine melanoma cells (RRID:CVCL_DN28) were obtained from Dr. Dawn Duval as part of the FCC Canine Cancer Cell Line Panel (Colorado State University, Fort Collins, CO, USA).[21] Both cell lines were grown in Dulbecco's Modified Eagle Medium (DMEM) (Life Technologies, Carlsbad, CA) containing 10% fetal bovine serum (FBS) (Gemini Biosciences, Sacramento, CA). WM115 (RRID:CVCL_0040) and HeLa (RRID:CVCL_0030) cells were obtained through American Tissue Type Collection (ATCC, Manassas, VA) and maintained in alpha-Minimal Essential Media (Life Technologies) or DMEM containing 10% FBS, respectively. All cell lines were maintained at 37°C and 5% CO_2 in a humidified incubator and passaged every 3 days or when confluency reached 80–90%.

To generate drug resistant UCDK9M4 cells lines, we cultured cells in the presence of 2.5 or 5 μM cisplatin over time. Fresh cisplatin was added at every media change or passage for a period of several weeks, at which time cells displayed growth despite the presence of drug.

All cell lines used in this study were previously established and validated. Jones, WM115, and HeLa cell lines were not subjected to specific verification testing in our laboratory; however, all cell lines were evaluated for morphology and maintenance of growth characteristics throughout this study. UCDK9M2 and M4 cell lines were sourced from the original stocks which have been validated to be of canine origin without interspecies contamination using a commercial laboratory (Idexx Radil, Colombia, MO). All cell lines tested free of mycoplasma using MycoFluor (Life Technologies) and/or PCR-based methods.

2.2 | Canine tissue sourcing

Canine oral and lingual melanoma samples were collected from live patients at the time of biopsy or tumour removal, evaluated by a boarded pathologist, and banked by University of California, Davis, School of Veterinary Medicine. Samples were collected prior to any chemo-, radiation-, or immuno-therapy and randomly selected from the tumour bank for use in this study.

2.3 | Sequence alignment

Amino acid sequence analysis was performed using the publicly available sequences from the National Center for Biotechnology Information and aligned using Vector NTI software (Life Technologies).

2.4 | Cell lysis and western blotting

For measurement of caspase cleavage, UCDK9M4 cells were plated on tissue culture dishes and grown for 24 h before treatment with (DMSO) vehicle, doxorubicin (Selleck Chemicals, Houston, TX), or 2,4-pyridinedicarboxylic acid (2,4-PDCA) (Sigma–Aldrich, St. Louis, MO). Cells were incubated for an additional 24 hours following drug addition, then lysed as described below.

For measurement of JARID1B and cleaved-caspase 3, the indicated cells were lysed in RIPA buffer (Sigma–Aldrich) containing phosphatase and protease inhibitor cocktails, and 1 mM DTT for 20 min on ice. Lysates were then centrifuged for 15 min at 16000xg and the supernatant was collected. Protein concentration was measured using a DC protein assay (Bio Rad, Hercules, CA). A total of 40 μg of lysate (per well) was electrophoresed and transferred using standard protocols. Primary antibodies including anti-JARID1B, antitubulin, anti-actin, or anti-cleaved caspase 3 were used at a concentration of 1:500 to 1:2500. See antibody validation statements in Materials and Methods Section 2.7 for catalogue numbers and supplier information.

2.5 | Experimental procedures for drug treatment and irradiation experiments

For the imaging-based assays described below, cell lines were plated onto collagen I coated 96-well glass bottomed imaging plates (CellVis, Mountain View, CA) at a density of 4000 cells/well for UCDK9M2, M4, and WM115 cell lines or 500 cells/well for more rapidly dividing Jones cells. Cells were cultured overnight under standard conditions before the addition of drug.

2.5.1 | Cell survival experiments—Drug dilution series were prepared in complete cell line-specific growth media and added to cells the next morning in triplicate. Cisplatin (Selleck Chemicals) was prepared in sterile deionized water. Histone demethylase inhibitors, including 2,4-PDCA, 2-(4-Methylphenyl)- 1,2-benzisothiazol-3(2H)-one (PBIT), KDOAM-25 (Sigma–Aldrich), or CPI-455 (Selleck Chemicals) were prepared in DMSO. Each compound was evaluated for cytotoxic effects across the indicated range of concentrations. An equivalent amount of solvent (water or DMSO) was included in vehicle control wells for all experiments. Following drug addition, cells were grown for an additional 24–72 h, fixed, and processed as described in Materials and Methods Section 2.6.

2.5.2 | Cell irradiation experiments—Cells were plated using the methods described in this section, pretreated with vehicle or PDCA at the indicated concentrations for 2 h, then exposed to 6 MV photons from a linear accelerator using either a TrueBeam or a Varian 2100C (Varian Medical, Palo Alto, CA). For irradiation, cells were placed on 1.5 cm of superflab to act as bolus and treated from an angle of 180° to allow full build-up of dose to

the bottom of the plate. Cells were then fixed and processed at the indicated time points as described in Materials and Methods Section 2.6.

2.5.3 | Drug synergy experiments—Cells were plated as described in this section and equal volumes of cisplatin (0–40 μM) and PBIT (0–24 μM) were combined at different concentrations to create 64 total drug combinations to evaluate synergism, additivity, or antagonism. Cells were grown for 48 h after drug addition, then processed as described in Materials and Methods Section 2.6. Synergy experiments were repeated in duplicate for UCDK9M4 and Jones cell lines.

2.6 | Fixation and immunofluorescence staining

For drug treatment and irradiation experiments, cells were fixed with 4% paraformaldehyde (PFA) diluted in phosphate buffered saline (PBS) pH 7.2 for 20 min at room temperature. Cells were then rinsed with PBS and nuclei were stained with Hoechst 33342 diluted 1:10 000 in PBS for 10 min at room temperature, before finally washing into PBS for imaging.

For immunofluorescence experiments, cells were fixed as indicated above, followed by permeabilization with 1% Triton X-100 in PBS for 10 min, and blocked in PBS containing 2% bovine serum albumin (BSA) and 0.1% Triton (“blocking buffer”) for 1 h at room temperature. Primary antibodies were then diluted in blocking buffer at 1:200 for mouse anti-JARID1B and rabbit antiH3K4me3, 1:200 or 1:500 for rabbit anti-Ki67, and 1:500 for mouse anti-p-γH2AX, rabbit anti-p53BP1, and rabbit anti-Rad51 antibodies. Primary antibodies were incubated overnight at 4°C then rinsed three times with 0.1% Triton X-100 in PBS. Secondary antibodies, Alexa Fluor 546 or 647 (Molecular Probes, Eugene, OR), were diluted 1:200 in blocking buffer and incubated for 1 h at room temperature. Cells were then rinsed three times in PBS, incubated in Hoechst as indicated, and placed in fresh PBS for imaging.

For canine tissue immunofluorescence experiments, 5 μm thick sections were cut from OCT embedded fresh frozen tissues and mounted on slides. The slides were then thawed for 2 min at room temperature and fixed, permeabilized, and stained as indicated for cell culture experiments in this section, with the following exception: tissue sections were fixed with 3.7% PFA for 20 min instead of 4% PFA for 20 min.

2.7 | Antibody validation statement

JARID1B antibodies (ab244220, Abcam, Cambridge, MA) were validated by epitope sequence conservation, predicted mobility by western blotting, and localization by immunofluorescence. Ki67 (ab15580), tubulin (ab7291), H3K4me3 (ab8580, Abcam), p-γH2AX (05–636), actin (Sigma Aldrich), cleaved-caspase 3 (S9661), p53BP1 (S4937, Cell Signalling Technologies), and Rad51 (a kind gift from the W.D. Heyer lab, University of California, Davis) antibodies were validated by epitope sequence conservation, localization, predicted response by immunofluorescence, and/or predicted molecular weight and response by western blot.

2.8 | Image acquisition

Cells and tissues were imaged on a Nikon Ti2 inverted wide-field microscope, controlled by NIS-Elements software, (Nikon Instruments Inc, Melville, NY) fitted with Plan Apo 20x (NA = 0.75) and 60x (NA = 1.4) oil immersion lenses, a Sola II multi-wavelength LED excitation source (Lumencor, Beaverton, OR), and Prime 95B CCD camera (Photometrics, Tucson, AZ). For cell survival experiments, whole-well tiled imaging was performed to ensure accurate cell counts.

2.9 | Data analysis and statistics

Analysis of fluorescence intensity, cell counts, and statistics were performed using the custom MATLAB (MathWorks, Natick, MA) software as described previously.[22] For drug treatment experiments, cell survival fraction was determined as the number of Hoechst positive, non-apoptotic nuclei (regular nuclear border, maintenance of uniformity and circularity) relative to vehicle control. All experiments were conducted in triplicate and repeated at least three times, with an $n > 500$ cells per condition, unless otherwise indicated. Where appropriate, data were tested for normality using Kolmogorov-Smirnov and Anderson-Darling statistics. For datasets with non-normal distributions, significance was determined by Wilcoxon rank sum test, while normally distributed paired comparisons were evaluated by a two- sided *t*-test. In both cases, data were considered significant at a *p*-value of <.05. The SynergyFinder (version 2.0) web-application was used to evaluate drug interactions between cisplatin and PBIT in synergy experiments.[23] Synergy scores from three models (Bliss, Loewe, and Zero Interaction Potency [ZIP] models) were generated using this software, where a synergy score < −10 indicated antagonistic, from −10 to 10 additive, and > 10 a synergistic interaction. Data will be made upon reasonable request to the corresponding author.

3 | RESULTS

3.1 | Histone demethylase inhibitors modulate methylation status and radiation response in canine oral melanoma cell lines

Therapeutic targeting of tumour epigenetic regulation has been proposed to enhance therapeutic response, reduce acquired drug resistance, and/or directly induce cell death.[16,24,25] Based on these reports, we explored the utility of HDIs in canine oral melanoma cell lines as a single agent or combined with ionizing radiation. We used UCDK9M2 and UCDK9M4 (hereafter M2 and M4, respectively) canine oral melanoma cell lines that were previously derived from patient biopsy samples and extensively characterized.[19,20] As an initial proof-of-principal, we used 2,4-PDCA, hereafter referred to as PDCA, to inhibit demethylase activity. PDCA is an early generation, broad specificity HDI that binds to the catalytic core of many histone demethylases, including both H3K4 and H3K9 demethylases.[26] Consistent with these reports, we found that addition of PDCA increased H3K4 and H3K9 methylation (Figure 1(A)).

Upon treatment of M2 and M4 cell lines, we found a moderate, dose-dependent reduction in cell number with ~65–75% of cells surviving at the highest PDCA concentration tested (6.5 mM) relative to vehicle control (Figure 1(B)). When combined with ionizing radiation,

we found that pretreatment of cells with PDCA further reduced survival in a statistically significant manner (Figure 1(B)). These findings suggested that treatment with this HDI may directly modulate the cellular response to ionizing radiation. To evaluate this hypothesis, we stained M2 and M4 cell lines for DNA damage markers, p53BP1 and p-γH2AX, at 0, 2, 4, and 24 h time points following irradiation (Figure 1(C)). We found that PDCA delayed the resolution of DNA damage markers suggesting a delay in repair kinetics. We found this effect to be most prominent at 24 h post-irradiation in both M2 and M4 cells (p-value <.05, Wilcoxon rank sum test); with a greater magnitude in M4 cells (Figure 1(D),(E)) likely representing inter-cell line variation. Additionally, we noted a modest increase in p-γH2AX and p53BP1 foci at 0 h time points (relative to irradiation), indicating an effect of this compound on acquisition and/or repair of spontaneous damage (Figure 1(D),(E)). Staining for damage repair protein Rad51 revealed a strong correlation with p-γH2AX staining suggesting persistence of repair machinery at these sites and further supporting the hypothesis that PDCA down modulates damage repair efficiency (Figure 1(F)). Furthermore, we found that cell death under these conditions appeared to be predominantly caspase-3-independent as opposed to doxorubicin, which induced strong caspase-3 cleavage (Figure 1(G)) within 24 h. We interpreted these findings to mean that PDCA enhances cell death through caspase-3-independent apoptosis, mitotic catastrophe, or another caspase-independent mechanism, which are all commonly seen following exposure to ionizing radiation.[27] Altogether, these results indicated that inhibition of histone demethylase activity has direct and adjunctive anti-tumour properties. However, given the broad specificity of PDCA, this effect may be due to either inhibition of a specific demethylase or from inhibition of a set of multiple demethylases.

3.2 | JARID1B is a highly conserved histone H3K4 demethylase expressed in proliferating canine melanoma tissues

To investigate specific histone demethylase targets of PDCA which could account for the observed reduction in survival and modulation of radiation response in treated cells, we evaluated the JARID1 class of H3K4 demethylases which is composed of functionally redundant JARID1A/ 1B/ 1C/ 1D proteins.[16] We focused on this class of demethylases because JARID1B has been linked to tumorigenesis, therapy resistance, and/or altered cell cycle regulation in human melanoma and a number of other cancers.[10,11,28–30] We first assessed the level of primary sequence conservation between human and canine JARID1B. Analysis of the published sequence information (NCBI) indicated that canine JARID1B is slightly longer than human JARID1B with 1768 vs 1544 amino acids, respectively (Figure 2(A)). At the primary amino acid sequence level there was 88% homology. Within the JmjC domain, which is the functional domain catalysing histone demethylation, there was 100% amino acid sequence homology between human and canine JARID1B (Figure 2(A)). The three PHD domains displayed high sequence homology whereas the JmjN domain, which has been implicated in protein stability, was least conserved at 20% homology (Figure 2(A), (B)). These data indicated that canine JARID1B has a high degree of similarity as compared to the human form of this protein.

We validated the ability of commercially available antibodies to detect JARID1B expression in canine cell lines (see Materials and Methods, Section 2.7). Immuno-staining of fixed

canine melanoma cells revealed a nuclear localization pattern (Figure 2(C)) consistent with the reported localization of JARID1B in human cell lines.[16] In agreement with these results, we found that western blot for JARID1B detected a band corresponding to the predicted mobility of this protein from both canine melanoma and human cell lysates (Figure 2(D)), further validating the function of this antibody in canine samples.

To determine expression in patients, canine oral melanoma biopsy tissues were obtained from archived samples in the University of California, Davis, School of Veterinary Medicine tumour bank. Five treatment naive patient samples were obtained, one representing a lingual melanoma, and four from an oral location, with varying levels of pigmentation (Figure 3(A)). With the exception of the lingual tumour sample, metastatic disease was detected at the time of biopsy indicating the presence of aggressive disease in at least four out of five patients. All samples were analysed for JARID1B expression by immunofluorescence microscopy using the validated antibody (Figure 3(B)) versus a negative control consisting of secondary antibody only. In contrast to the reported immuno-histochemical findings in human tumour samples where JARID1B+ cells are infrequent,[10] JARID1B expression was detected in nearly all cells populating each tumour in three of the canine patient samples (Figure 3(B)). In the remaining two samples, the frequency of positive cells was qualitatively lower and mean signal intensities modestly reduced, but still readily detectable and widely distributed throughout the samples (Figure 3(B),(C)). These findings may reflect reduced density of tumour cells in these samples, variation in tissue specimen quality, or biological variation amongst patients. Nevertheless, we found that JARID1B is expressed with relatively high frequency in canine melanoma when compared to reports from human patients.

Reports from human melanoma indicate that JARID1B expression is anti-correlated with proliferation.[8] By contrast, our finding that JARID1B expression is widespread in aggressive tumour samples suggested that the expression-proliferation relationship is different in canine oral melanomas. To test this hypothesis, we assessed the fraction of actively proliferating cells within each patient by measuring Ki67 levels, finding a mean positivity range of ~5%–25% of the total cell population amongst the tumour samples (Figure 3(D)). To rule out the possibility that JARID1B and Ki67 expression are anti-correlated at the single cell level, as would be expected from human melanoma studies, we performed co-staining experiments. Our analysis revealed that within the canine patient samples, JARID1B expression was present in nearly all cells irrespective of Ki67 expression status (Figure 3(E)). To quantitatively assess this relationship, we performed a linear regression analysis which revealed a moderate level of correlation between single cell Ki67 and JARID1B expression ($R^2 = 0.59$, Figure 3(F)). Based on these data, we concluded that Ki67 and JARID1B can be co-expressed (Figure 3(E), see arrowheads) and positively correlated with the ability of cells to proliferate in canine tissues (Figure 3(F)) unlike human melanoma tissues.

3.3 | HDIs with enhanced JARID1 specificity and potency reduce cell survival without altering radiation response kinetics

We next aimed to determine if inhibition of JARID1 demethylases could account for reductions in cell survival and the enhanced radiosensitivity observed when cells were treated with PDCA (Figure 1(B)). To this end, we evaluated the dose dependent cytotoxicity of CPI-455, PBIT (2-(4-Methylphenyl)-1,2-benzisothiazol-3(2H)-one), and KDOAM-25 in M4 cells relative to cisplatin.[31–33] Although no JARID1B-specific inhibitors were available, the three inhibitors evaluated have reported selectivity for JARID1 family H3K4 demethylases, making them pan-JARID1 inhibitors. To test their effectiveness, cells were treated with a wide range of concentrations (nM to μM) for each drug and the survival fraction was measured relative to vehicle treated conditions. Potency varied amongst the inhibitors, generally requiring μM concentrations to achieve reduction in cell survival (Figure 4(A)).Although more efficacious than PDCA at reducing cell survival fractions, KDOAM-25 and CPI-455 inhibitors still required concentrations at or exceeding 50 μM to induce significant reductions in cell number, despite their reported nanomolar IC_{50} values (Figure 4(A)). However, PBIT showed more promise, exhibiting reductions in survival in the low μM range consistent with its reported IC_{50} range. Repetition of the cell death assay consistently resulted in less than 50% survival at 24 μM and less than 10% survival at 48 μM PBIT treatment (Figure 4(A)). We verified that PBIT was effective in other oral melanoma cell lines and found it to be even more potent in the rapidly proliferating Jones canine melanoma cell line (Figure 4(B)). By comparison, PBIT was significantly less effective at reducing cell survival fractions in the human melanoma cell line WM115 under the same conditions (Figure 4(C)).

Based on these results, we tested the effectiveness of PBIT in combination with ionizing radiation or cisplatin. Unlike PDCA, we found that PBIT in combination with irradiation did not have any additive or synergistic properties (data not shown). Similarly, PBIT in combination with cisplatin only synergized at the highest combinations of drug (Supplemental Figure 1). These results implied a separation of function where inhibition of JARID1 demethylases is limited to cell survival whereas broad spectrum histone demethylase inhibition (ie, PDCA) effects both cell survival and response to DNA damage. Nevertheless, our results showed strong dose-dependent anti-cancer properties for JARID1-targeted HDIs.

3.4 | PBIT reduces cell survival in cisplatin- resistant canine melanoma cell lines

Potentially efficacious as a single agent, we next considered whether PBIT could be used in the case of resistance to standard of care therapies. To this end, we generated two cisplatin-resistant M4 cell lines by continuous exposure to low-dose cisplatin (see Materials and Methods, Section 2.1). Once cell lines exhibited regrowth in the presence of cisplatin, they were considered resistant and used in our assays. In control cells (non-resistant), both cisplatin and PBIT (Figure 5(A)) killed cells in a dose-dependent manner, with almost a 100% reduction in cell survival relative to vehicle treated cells occurring near 50 μM for each drug as seen in our previous experiments (Figure 4(A)). In contrast, cell lines continuously grown in 2.5 μM (Figure 5(B)) or 5 μM (Figure 5(C)) cisplatin showed 30% and 70% cell survival, respectively, when treated with 50 μM cisplatin. This drastic increase

in cell survival after cisplatin treatment confirmed that the two cisplatin-resistant cell lines were indeed platinum-resistant relative to control cells. Importantly, when cisplatin-resistant cell lines were challenged with PBIT, the inhibitor retained its effectiveness (Figure 5(B), (C)). These data suggested that PBIT may serve as a potent drug for canine melanoma exhibiting resistance to cisplatin, with nearly a 100% reduction in survival achievable in cell culture studies.

4 | DISCUSSION

Histone demethylase inhibitors (HDIs) have been widely explored as anti-cancer treatments due to their abilities to modulate cell proliferation, DNA damage responses, and the acquisition of therapy resistant phenotypes. Here we show that broad spectrum HDIs induce a moderate reduction in cell survival *and* modulate DNA damage responses in canine oral melanoma cell lines. A more refined analysis of HDIs specifically targeting the JARID1 family of histone demethylases (PBIT) revealed a significant effect on cell survival, but no evidence of a role in modulating DNA damage responses. These data support a separation of function between pan-JARID1 inhibitors vs broad spectrum HDIs. Thus, inhibition of JARID1 family members may prove most effective in a single drug setting, as indicated by our results demonstrating a preserved sensitivity to PBIT in cell resistance to cisplatin (Figure 5(B),(C)). Alternatively, inhibition of other demethylases, particularly H3K9-targeted demethylases that are reported to modulate damage response, may be useful in combination with radiation or cytotoxic agents.

Interestingly, we found that HDIs result in a modest but statistically significant increase in H3K4 methylation (Figure 1(A)) yet a significant reduction in cell survival. In light of these results, it is possible that HDIs may affect the regulation of only a small set of genes, but those genes are critical for cell survival. In agreement with this hypothesis, reports show that H3K4 methylation status only effects the transcription of a small number of genes, nevertheless, deletion of JARID1 family members causes embryonic lethality.[16,34,35] Adding an additional layer of complexity, studies in human breast cancer demonstrate that promoter occupancy by JARID1B (and other histone demethylases) alone is not sufficient to drive promoter demethylation because its function is modulated by additional proteins, for example, androgen receptor and several transcription-associated proteins.[36,37] Thus, diffuse association of these demethylases with chromatin is not enough to render them enzymatical active at a global level. In the context of our results, we infer that JARID1 family members regulate small changes in chromatin state that have a profound impact on cell survival in canine melanoma cells.

An important consideration is that our results may reflect nonchromatin, off-target effects which could also contribute to the observed cell death effects, especially at the highest concentrations of inhibitors tested in our assays. This possibility emphasizes the need for additional studies to provide a deeper insight into the functions of JARID1 in canine oral melanoma, and cancer more generally. Such exploration would afford the opportunity to develop increasingly targeted therapeutic approaches, perhaps aimed specifically at an important subset of targets downstream of JARID1, or to uncover important off-target effects of these compounds.

As a whole, our results in canine oral melanoma cell lines are inconsistent with the role of JARID1 family members as reported by Roesch et al for human melanoma.[10] JARID1B is more diffusely expressed and positively correlated with proliferative tumours in canine melanoma patients, as opposed to the observation of rare JARID1B+ cells in human melanomas where its expression is associated with dormancy.[10] These results argue that canine oral melanoma behaves in a distinct manner as compared to human melanoma with regard to JARID1B. These findings are not entirely surprising as canine oral melanoma and human cutaneous melanomas are distinct diseases with different drivers.[38,39] For example, *BRAF* V600E mutations in human melanoma are not commonly seen in canine oral melanoma, and we find that human melanoma cells are less sensitive to PBIT as compared to canine cells. By comparison, however, JARID1B function in canine oral melanoma appears to be more similar to its role in human breast, oesophageal, and prostate cancers where its expression is associated with aggressive disease.[30,36,40] Given the known association between JARID1B in development and differentiation, it is interesting to speculate that JARID1B expression in canine oral melanoma may contribute to the maintenance of a poorly differentiated cell state, which is a hallmark of aggressive tumours.[15,17,20,37] This may represent at least a partial link between the high levels of demethylase expression, rapid disease progression, and therapy resistance observed in canine oral melanomas. Measurement of JARID1B expression, or that of other family members, may therefore provide a useful gauge to assess the aggressiveness of an individual tumour and guide treatment strategies for canine patients.

Further work is needed in both human and canine cancers to more fully understand the role of JARID1B, its family members, and other histone demethylases in cancer and the potential efficacy of targeting these proteins in cancer treatment. However, despite these future challenges, our findings demonstrate proof-of-principle for the use of HDIs in canine oral melanoma as a primary therapeutic agent or in cases of cytotoxic drug resistance and establish the foundation for additional studies.

Supplementary Material

Refer to Web version on PubMed Central for supplementary material.

ACKNOWLEDGEMENTS

We would like to thank members of the Davies and Kent laboratories for their helpful input and suggestions. We would also like to thank Drs. Wessel Dirksen and William Kisseberth for kindly sharing resources to complete this study.

Funding information

Morris Animal Foundation- Pfizer Animal Health Fellowship, Grant/Award Number: D10MS-906; National Cancer Institute, Grant/Award Number: T32 CA251007; The Ohio State University Comprehensive Cancer Center and the National Institutes of Health, Grant/Award Number: P30 CA016058; Toni Wiebe Memorial Research Fund

REFERENCES

1. Smedley RC, Spangler WL, Esplin DG, et al.Prognostic markers for canine melanocytic neoplasms: a comparative review of the literature and goals for future investigation. Vet Pathol. 2011;48: 54–72. [PubMed: 21266721]

2. Atherton MJ, Morris JS, McDermott MR, Lichty BD. Cancer immunology and canine malignant melanoma: a comparative review. Vet Immunol Immunopathol. 2016;169:15–26. [PubMed: 26827834]

3. Prouteau A, Chocteau F, Brito C, et al.Prognostic value of somatic focal amplifications on chromosome 30 in canine oral melanoma. Vet Comp Oncol. 2020;18:214–223. [PubMed: 31461207]

4. van der Weyden L, Brenn T, Patton EE, Wood GA, Adams DJ. Spontaneously occurring melanoma in animals and their relevance to human melanoma. J Pathol. 2020;252:4–21. [PubMed: 32652526]

5. Dasari S, Tchounwou PB. Cisplatin in cancer therapy: molecular mechanisms of action. Eur J Pharmacol. 2014;740:364–378. [PubMed: 25058905]

6. Nair N, Shoaib M, Sorensen CS. Chromatin dynamics in genome stability: roles in suppressing endogenous DNA damage and facilitating DNA repair. Int J Mol Sci. 2017;18:1486.

7. Glasspool RM, Teodoridis JM, Brown R. Epigenetics as a mechanism driving polygenic clinical drug resistance. Br J Cancer. 2006;94:10871092.

8. Greer EL, Shi Y. Histone methylation: a dynamic mark in health, disease and inheritance. Nat Rev Genet. 2012;13:343–357. [PubMed: 22473383]

9. Kang MK, Mehrazarin S, Park NH, Wang CY. Epigenetic gene regulation by histone demethylases: emerging role in oncogenesis and inflammation. Oral Dis. 2017;23:709–720. [PubMed: 27514027]

10. Roesch A, Fukunaga-Kalabis M, Schmidt EC, et al.A temporarily distinct subpopulation of slow-cycling melanoma cells is required for continuous tumor growth. Cell. 2010;141:583–594. [PubMed: 20478252]

11. Roesch A, Vultur A, Bogeski I, et al.Overcoming intrinsic multidrug resistance in melanoma by blocking the mitochondrial respiratory chain of slow-cycling JARID1B(high) cells. Cancer Cell. 2013;23:811–825. [PubMed: 23764003]

12. Young LC, McDonald DW, Hendzel MJ. Kdm4b histone demethylase is a DNA damage response protein and confers a survival advantage following gamma-irradiation. J Biol Chem. 2013;288:21376–21388. [PubMed: 23744078]

13. Almeida LO, Abrahao AC, Rosselli-Murai LK, et al.NFkappaB mediates cisplatin resistance through histone modifications in head and neck squamous cell carcinoma (HNSCC). FEBS Open Bio. 2014;4: 96–104.

14. Takata H, Hanafusa T, Mori T, et al.Chromatin compaction protects genomic DNA from radiation damage. PLoS One. 2013;8:e75622. [PubMed: 24130727]

15. Dey BK, Stalker L, Schnerch A, Bhatia M, Taylor-Papidimitriou J, Wynder C. The histone demethylase KDM5b/JARID1b plays a role in cell fate decisions by blocking terminal differentiation. Mol Cell Biol. 2008;28:5312–5327. [PubMed: 18591252]

16. Harmeyer KM, Facompre ND, Herlyn M, Basu D. JARID1 histone demethylases: emerging targets in cancer. Trends Cancer. 2017;3:713–725. [PubMed: 28958389]

17. Schmitz SU, Albert M, Malatesta M, et al.Jarid1b targets genes regulating development and is involved in neural differentiation. EMBO J. 2011;30:4586–4600. [PubMed: 22020125]

18. Fan L, Xu S, Zhang F, et al.Histone demethylase JMJD1A promotes expression of DNA repair factors and radio-resistance of prostate cancer cells. Cell Death Dis. 2020;11:214. [PubMed: 32238799]

19. Aina OH, Maeda Y, Harrison M, et al.Canine malignant melanoma alpha-3 integrin binding peptides. Vet Immunol Immunopathol. 2011; 143:11–19. [PubMed: 21722969]

20. Zhang J, Chen X, Kent MS, Rodriguez CO, Chen X. Establishment of a dog model for the p53 family pathway and identification of a novel isoform of p21 cyclin-dependent kinase inhibitor. Mol Cancer Res. 2009;7:67–78. [PubMed: 19147538]

21. Yoshikawa H, Sunada S, Hirakawa H, et al.Radiobiological characterization of canine malignant melanoma cell lines with different types of ionizing radiation and efficacy evaluation with cytotoxic agents. Int J Mol Sci. 2019;20:841.

22. Davies AE, Pargett M, Siebert S, et al.Systems-level properties of EGFR-RAS-ERK signaling amplify local signals to generate dynamic gene expression heterogeneity. Cell Syst. 2020;11:161–175. [PubMed: 32726596]

23. Ianevski A, Giri AK, Aittokallio T. SynergyFinder 2.0: visual analytics of multi-drug combination synergies. Nucleic Acids Res. 2020;48:W488W493.
24. Sharma SV, Lee DY, Li B, et al.A chromatin-mediated reversible drug-tolerant state in cancer cell subpopulations. Cell. 2010;141:69–80. [PubMed: 20371346]
25. Risom T, Langer EM, Chapman MP, et al.Differentiation-state plasticity is a targetable resistance mechanism in basal-like breast cancer. Nat Commun. 2018;9:3815. [PubMed: 30232459]
26. Kristensen LH, Nielsen AL, Helgstrand C, et al.Studies of H3K4me3 demethylation by KDM5B/Jarid1B/PLU1 reveals strong substrate recognition in vitro and identifies 2,4-pyridine-dicarboxylic acid as an in vitro and in cell inhibitor. FEBS J. 2012;279:1905–1914. [PubMed: 22420752]
27. Eriksson D, Stigbrand T. Radiation-induced cell death mechanisms. Tumour Biol. 2010;31:363–372. [PubMed: 20490962]
28. Barrett A, Santangelo S, Tan K, et al.Breast cancer associated transcriptional repressor PLU-1/JARID1B interacts directly with histone deacetylases. Int J Cancer. 2007;121:265–275. [PubMed: 17373667]
29. Tang DE, Dai Y, Fan LL, et al.Histone demethylase JMJD1A promotes tumor progression via activating snail in prostate cancer. Mol Cancer Res. 2020;18:698–708. [PubMed: 32019811]
30. Xiang Y, Zhu Z, Han G, et al.JARID1B is a histone H3 lysine 4 demethylase up-regulated in prostate cancer. Proc Natl Acad Sci U S A. 2007;104:19226–19231. [PubMed: 18048344]
31. Sayegh J, Cao J, Zou MR, et al.Identification of small molecule inhibitors of jumonji AT-rich interactive domain 1B (JARID1B) histone demethylase by a sensitive high throughput screen. J Biol Chem. 2013;288:9408–9417. [PubMed: 23408432]
32. Bavetsias V, Lanigan RM, Ruda GF, et al.8-Substituted pyrido[3,4-d] pyrimidin-4(3H)-one derivatives as potent, cell permeable, KDM4 (JMJD2) and KDM5 (JARID1) histone lysine demethylase Inhibitors. J Med Chem. 2016;59:1388–1409. [PubMed: 26741168]
33. Tumber A, Nuzzi A, Hookway ES, et al.Potent and selective KDM5 inhibitor stops cellular demethylation of H3K4me3 at transcription start sites and proliferation of MM1S myeloma cells. Cell Chem Biol. 2017;24:371–380. [PubMed: 28262558]
34. Catchpole S, Spencer-Dene B, Hall D, et al.PLU-1/JARID1B/KDM5B is required for embryonic survival and contributes to cell proliferation in the mammary gland and in ER+ breast cancer cells. Int J Oncol. 2011;38:1267–1277. [PubMed: 21369698]
35. Facompre ND, Harmeyer KM, Sole X, et al.JARID1B enables transit between distinct states of the stem-like cell population in oral cancers. Cancer Res. 2016;76:5538–5549. [PubMed: 27488530]
36. Yamamoto S, Wu Z, Russnes HG, et al.JARID1B is a luminal lineagedriving oncogene in breast cancer. Cancer Cell. 2014;25:762–777. [PubMed: 24937458]
37. Kidder BL, Hu G, Zhao K. KDM5B focuses H3K4 methylation near promoters and enhancers during embryonic stem cell self-renewal and differentiation. Genome Biol. 2014;15:R32. [PubMed: 24495580]
38. Wong K, Van der Weyden L, Schott CR, et al.Cross-species genomic landscape comparison of human mucosal melanoma with canine oral and equine melanoma. Nat Commun. 2019;10:353. [PubMed: 30664638]
39. Hodis E, Watson IR, Kryukov GV, et al.A landscape of driver mutations in melanoma. Cell. 2012;150:251–263. [PubMed: 22817889]
40. Kano Y, Konno M, Ohta K, et al.Jumonji/Arid1b (Jarid1b) protein modulates human esophageal cancer cell growth. Mol Clin Oncol. 2013;1:753–757. [PubMed: 24649241]

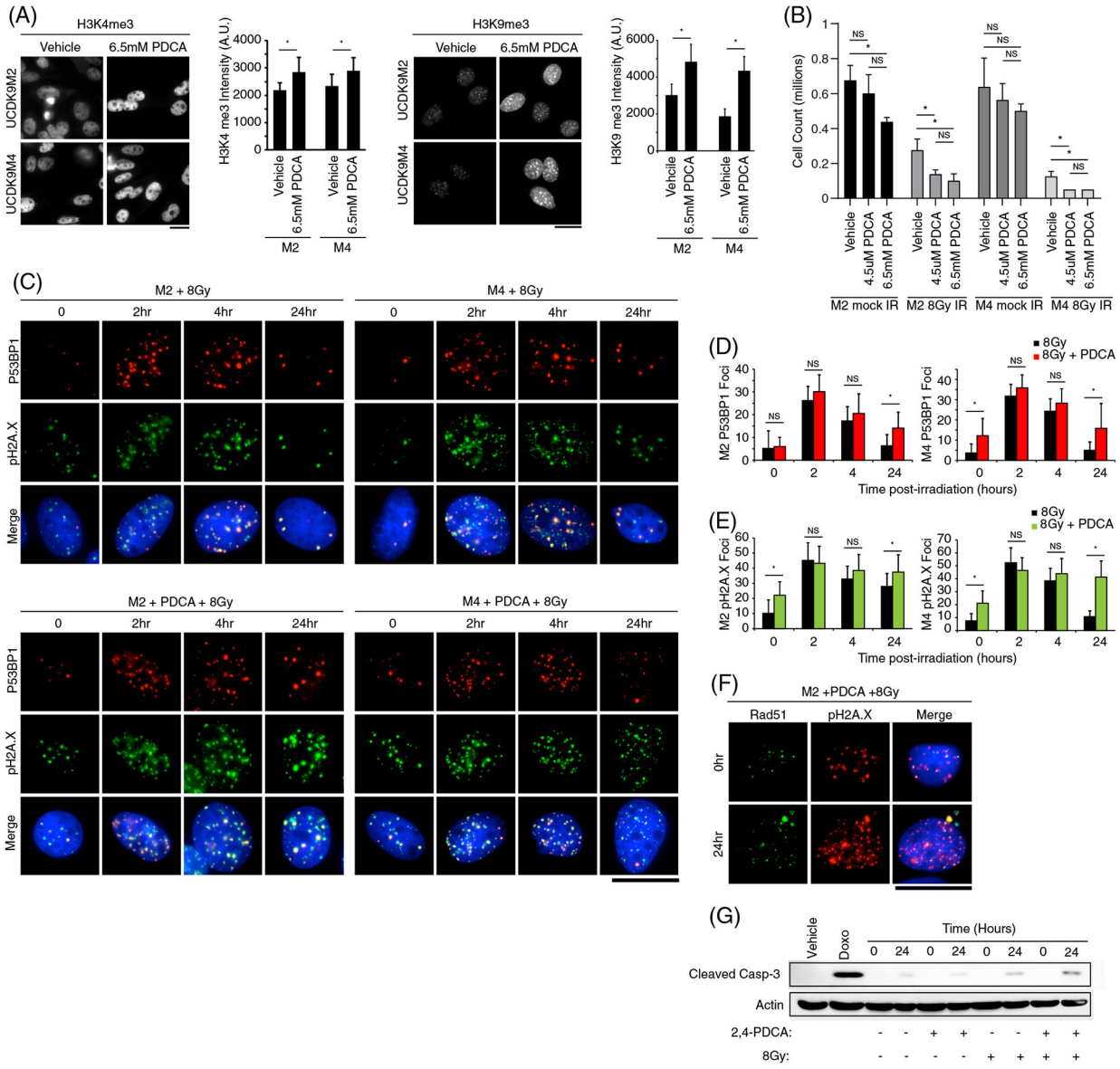

FIGURE 1.

Broad spectrum histone demethylase inhibition reduces cell survival and modulates DNA damage response kinetics.(A) Immunofluorescence data images and quantification of histone H3K4me3 (left) and H3K9me3 (right) in UCDK9M2 and M4 cell lines with or without 6.5 mM PDCA. H3K4 and H3K9 methylation signals are reported in arbitrary units (A.U.). Error bars represent the SD. Normality was determined as described in the methods, pairwise evaluations were then made using a two-sided *t*-test. *corresponds with *p*-value <.05. Scale bar 10 μM. (B) Column graphs representing M2 and M4 absolute cell count per condition (in millions of cells) following treatment with differing concentrations of PDCA, 8 Gy ionizing radiation, or both compared to vehicle control. Error bars represent the SD. Pairwise evaluations were made using a two-sided t-test. *corresponds with *p*-value <.05. N.S. = not significant. (C) Immunofluorescence images of cells treated with 8 Gy ionizing radiation or ionizing radiation plus 6 mM PDCA, fixed at the indicated time points in hours

post-treatment, and stained for p53BP1 (red), p- γH2AX DNA (green), and nuclei with Hoechst (blue). Scale bar 10 μM. (D-E) Number of p- γH2AX or p53BP1 foci counted per nuclei at the indicated time points for M2 and M4 cells under the indicated conditions. $n >$ 30 nuclei per time point. The distributions were determined to be non-normal as described in the methods; therefore, pairwise comparisons were made using the Wilcoxon rank sum test. *corresponds with p-value <.05. N.S. = not significant. (F) Immunofluorescence of cells exposed to 8 Gy ionizing radiation plus 6 mM PDCA co-stained for damage repair protein Rad51 (green), p- γH2AX (red), and nuclei with Hoechst (blue) 24 h post-treatment. Scale bar 10 μM. (G) Western blot for cleaved caspase-3 at 0 and 24 h time points following addition of the indicated compounds. Actin was used as a loading control, vehicle (DMSO) as a negative control, and doxorubicin as a positive control for caspase-3-mediated apoptosis

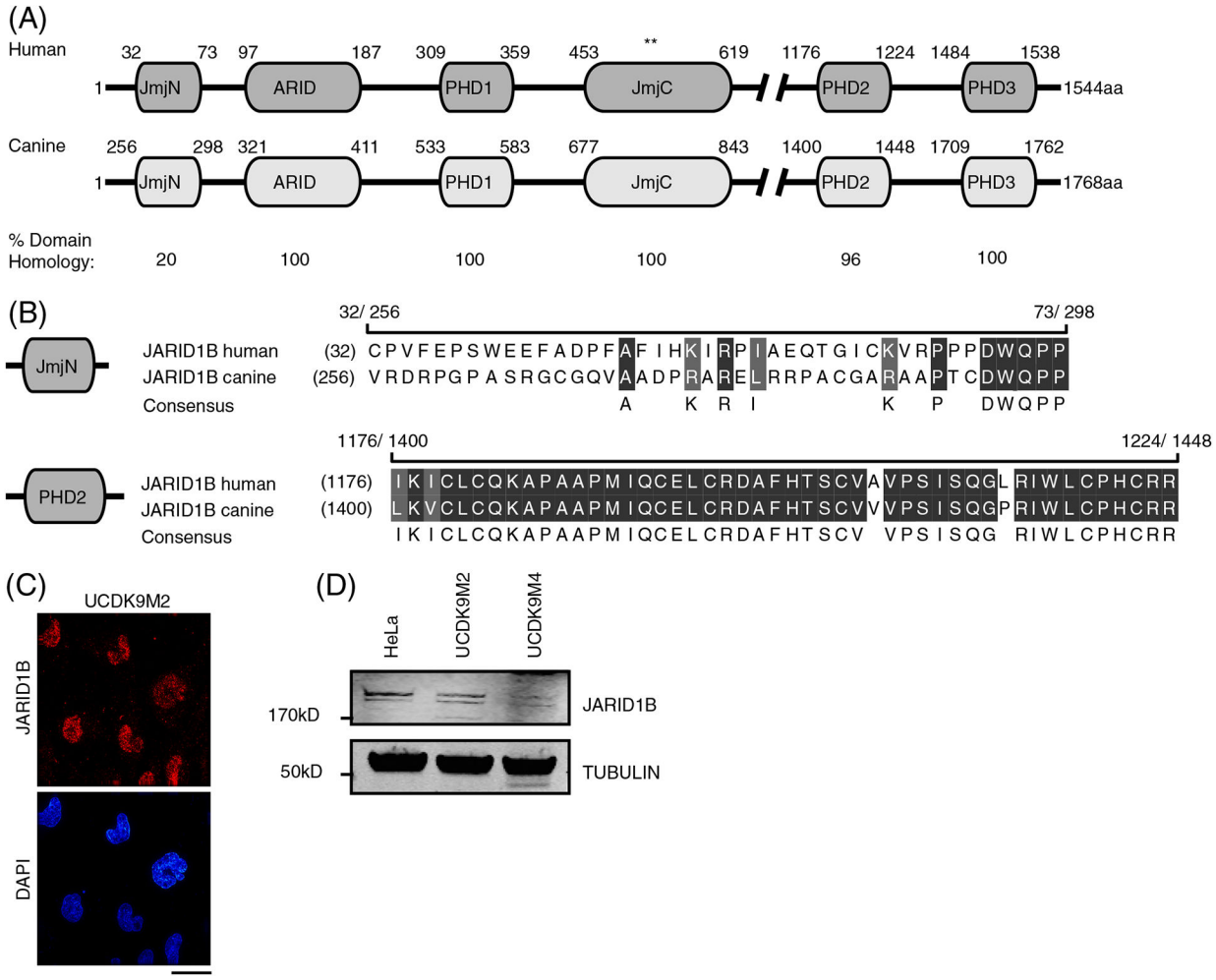

FIGURE 2.

Histone demethylase JARID1B is highly conserved and expressed in canine oral melanoma cells. (A) Domain alignment illustration comparing human and canine JARID1B using published sequence information. Superscripts represent relative amino acid positions of domain segments based on primary sequence alignment. Double asterisks (**) demarcate the JmjC histone demethylase domain. Numbers below the diagram indicate the percent homology within the indicated domain. (B) Diagram highlighting sequence differences in the JmjN and PHD2 domains where 20% and 96% homology exists, respectively, between human and canine JARID1B. Black shading denotes conserved, grey shading high similarity, and white non-conserved amino acids. (C) Immunofluorescence staining of M2 cell line with anti-JARID1B antibodies (red), nuclear staining with Hoechst (blue). Scale bar = 10 μM. (D) Western blot of JARID1B protein in human cell lysates (HeLa) as compared to M2 and M4 canine melanoma cells. Tubulin was used as a loading control

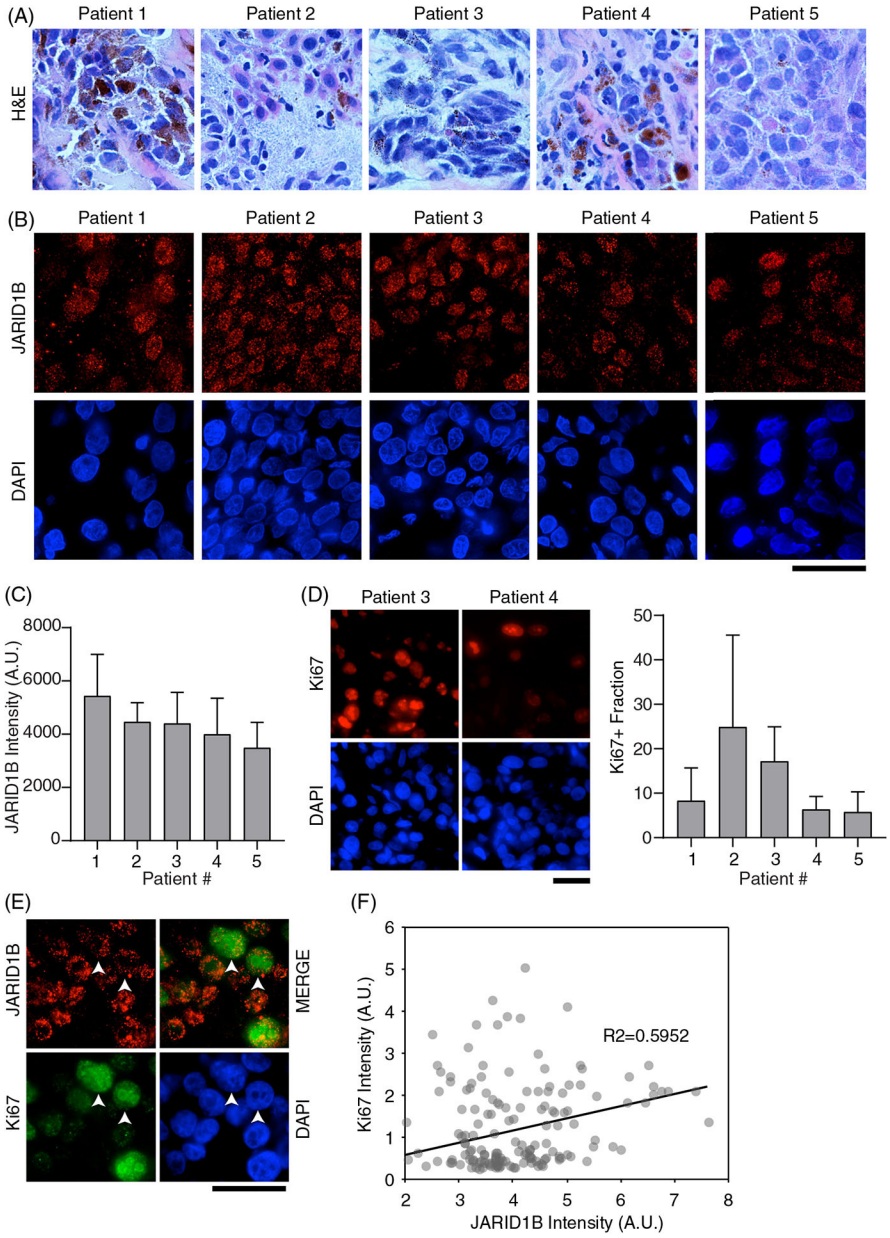

FIGURE 3.

JARID1B is highly expressed in canine oral melanoma tissues and is positively correlated with proliferation. (A) Five representative H&E stained canine melanoma biopsy samples from different patients. Tissue samples displayed melanin pigmentation that varied within and between the samples. All samples were evaluated by a boarded pathologist. (B) Immunofluorescence staining of JARID1B (red) and the nucleus with Hoechst (blue) in canine patient tissue samples corresponding with the tissues shown in Figure 3(A). Scale bar = 20 μM. (C) Column graph representing the integrated fluorescence intensity of JARID1B signal (reported in arbitrary units [A.U.]) obtained from five canine melanoma samples. Error bars represent the SD. (D) Representative immunofluorescent images of biopsy samples from patients 3 and 4 stained for Ki67 (red) and the nucleus with Hoechst

(blue). Column graph representing the average percentage of Ki67 positive cells per ×60 micrograph. Error bars represent the SD. Scale bar = 20 μM. (E) Representative images of tissues co-stained for JARID1B (red), Ki67 (green), a merge of JARID1B and Ki67 (green and red), or Hoechst (blue). Arrowheads indicate cells co-expressing JARID1B and Ki67. Scale bar = 20 μM. (F) Composite scatter plot and linear regression analysis of integrated nuclear Ki67 and JARID1B intensities obtained from patient Samples 1–5

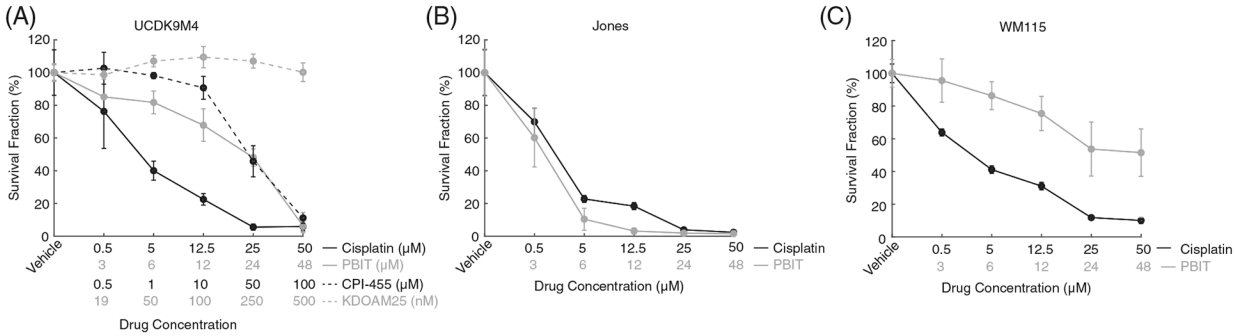

FIGURE 4.

JARID1-specific inhibitors reduce canine oral melanoma cell survival in a dose-dependent manner. (A) Line graph representing the survival fraction of M4 cells after treatment with cisplatin (μM), or pan-JARID1 histone demethylase inhibitors PBIT (μM), CPI-455 (μM), KDOAM 25 (nM) at the indicated concentrations. (B) Line graph representing the survival fraction of Jones canine melanoma cells after treatment with cisplatin or PBIT at the indicated concentrations. (C) Line graph of human WM115 melanoma cell line assessed for survival after treatment with cisplatin or PBIT treatment at the indicated concentrations. For all experiments, survival fraction was normalized relative to vehicle control and error bars indicate normalized SD

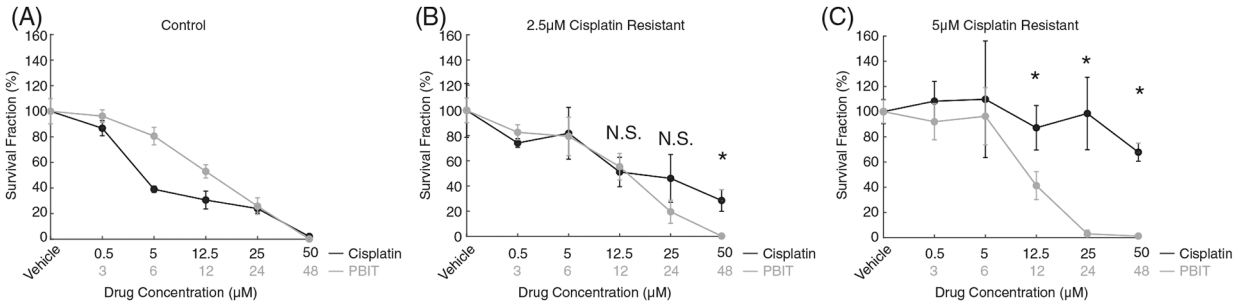

FIGURE 5.

Pan-JARID1 inhibitor PBIT effectively reduces cell survival in cisplatin resistant cell lines. (A) Line graph depicting the survival fraction of control (not cisplatin resistant) M4 cells treated with cisplatin or PBIT at the indicated concentrations of drug. (B) Line graph indicating the survival fraction of 2.5 μM cisplatin resistant M4 cell line, re-challenged with cisplatin or PBIT at the indicated concentrations of drug. (C) Line graph indicating the survival fraction of 5 μM cisplatin resistant M4 cell line, re-challenged with cisplatin or PBIT at the indicated concentrations of drug. For all experiments, survival fraction was normalized relative to vehicle control and error bars indicate normalized SD. Pairwise evaluations in (B-C) were made using a two-sided *t*-test. *corresponds with *p*-value <.05. N.S. = not significant